JMEPEG (2018) 27:2617–2621
DOI: 10.1007/s11665-017-3024-9

1059-9495/$19.00

Solar Light Responsive Photocatalytic Activity of Reduced Graphene Oxide–Zinc Selenide Nanocomposite

Koushik Chakraborty, Sk Ibrahim, Poulomi Das, Surajit Ghosh, and Tanusri Pal

(Submitted April 19, 2017; in revised form August 23, 2017; published online October 26, 2017)

Solution processable reduced graphene oxide–zinc selenide (RGO–ZnSe) nanocomposite has been successfully synthesized by an easy one-pot single-step solvothermal reaction. The RGO–ZnSe composite was characterized structurally and morphologically by the study of XRD analysis, SEM and TEM imaging. Reduction in graphene oxide was confirmed by FTIR spectroscopy analysis. Photocatalytic efficiency of RGO–ZnSe composite was investigated toward the degradation of Rhodamine B under solar light irradiation. Our study indicates that the RGO–ZnSe composite is catalytically more active compared to the controlled-ZnSe under the solar light illumination. Here, RGO plays an important role for photoinduced charge separation and subsequently hinders the electron–hole recombination probability that consequently enhances photocatalytic degradation efficiency. We expect that this type of RGO-based optoelectronics materials opens up a new avenue in the field of photocatalytic degradation of different organic water pollutants.

Keywords electronic materials, nanomaterials, semiconductors

1. Introduction

Recently, semiconductor nanostructures have been extensively studied because of their enormous potential applications as catalysts to tackle the serious environmental pollution (Ref 1, 2). Zinc selenide (ZnSe) an important II–IV direct band gap (E_g = 2.67 eV) semiconductor has been extensively investigated as a budding photocatalyst because of its low cost, ease of production, with high photochemical stability, and low toxicity (Ref 3, 4). However, the rapid recombination rate of photoinduced electron–hole inside the ZnSe nanostructure restricts its photocatalytic performance under visible light illumination. Several efforts have been paid to overcome this limitation by separating the electrons and holes efficiently (Ref 5, 6).

To this end, graphene, a two-dimensional honeycomb structure, is considered as a promising optoelectronic material because of its outstanding electronic and photonic properties with high electronic mobility (Ref 7-9). Most significantly, graphene has the capability to absorb photons over a broad spectrum from infrared to visible region. These extraordinary electronic and optical properties make graphene a potential optoelectronic material for the applications in light-emitting devices to touch screens, solar cells, ultrafast lasers and photodetectors (Ref 7-9). One of the efficient and scalable ways for solution processable synthesis of graphene is by the reduction in oxidized graphene, called reduced graphene oxide (RGO) (Ref 10). RGO has also established its impending candidateship in the field of optoelectronics, energy-storage devices and composite materials owing to its low-cost fabrication, mechanical flexibility, wide absorption band and compatibility with various substrates. In RGO-based nanocomposites, RGO provides the opportunities to enhance the intrinsic properties of the attached nanomaterials in diverse manners (Ref 11-14). Here, RGO plays the role of photocharge separator at the interface and offers continuous pathways for the electron transfer process. The capability to store and shuttle electrons builds RGO as an essential matrix element to the synthesis of RGO-based hybrid materials with improved photocatalytic activity in the direction of degradation of organic pollutants.

Nowadays, several efforts have been made to attach RGO with semiconductor photocatalysts to enhance the photocatalytic performance (Ref 12-16). The RGO–ZnSe composite exhibited remarkably enhanced photocatalytic activities toward the degradation of methylene blue (MB) dye under visible light irradiation (Ref 17-19). To our best knowledge all the reports are confined on the degradation of MB dye only (Ref 17-19). No report has been noticed on the use of RGO–ZnSe composite for the solar light responsive photocatalytic degradation of Rh B, a commonly used organic pollutant in textile industries.

Herein, we report the single-step synthesis of solution processable RGO–ZnSe composite by simple one-pot solvothermal process. The reduction in graphene oxide (GO), synthesis of ZnSe and attachment of ZnSe on RGO sheets occurs simultaneously. The as-synthesized composite was characterized both structurally and optically. The photocatalytic performance of the RGO–ZnSe toward the degradation of Rh B was investigated in detail. Our results demonstrate the significant role of RGO toward the enhancement of catalytic performances of the RGO-based hybrid nanocomposite.

This article is an invited paper selected from presentations at "ICETINN-2017, International Conference on Emerging Trends in Nanoscience and Nanotechnology," held March 16–18, 2017, in Majitar, Sikkim, India, and has been expanded from the original presentation.

Koushik Chakraborty, **Sk Ibrahim,** and **Surajit Ghosh**, Department of Physics and Technophysics, Vidyasagar University, Midnapore 721102, India; and **Poulomi Das** and **Tanusri Pal**, Department of Physics, Midnapore College, Midnapore 721101, India. Contact e-mail: tanusri.pal@gmail.com.

2. Experimental

2.1 Materials

Graphite powder, potassium persulfate [$K_2S_2O_8$], sodium nitrate [$NaNO_3$], sodium selenite [Na_2SeO_3], phosphorus pentoxide [P_2O_5], zinc acetate dihydrate [$Zn(CH_3COO)_2$, $2H_2O$], poly(vinylpyrrolidone) [PVP] were purchased from Sigma-Aldrich. 4-nitrophenol [$C_6H_5NO_3$; 4-NP], sulfuric acid [H_2SO_4], hydrogen peroxide [H_2O_2], potassium permanganate [$KMnO_4$], hydrochloric acid [HCl], ethylenediamine [$C_2H_8N_2$; ED], ethyleneglycol [$C_2H_6O_2$; EG] were purchased from Merck. All chemicals used in this experiment were of analytical grade and were used as received without further purification.

2.2 Materials Preparation

2.2.1 Synthesis of Graphene Oxide (GO). GO was synthesized by the oxidation of natural graphite powder via modified Hummers' method (Ref 16, 20). The detailed synthesis process has been published elsewhere (Ref 12, 16, 20).

2.2.2 Synthesis of RGO–ZnSe Nanocomposites, Controlled-ZnSe and Controlled-RGO. In a typical process, GO powder (40 mg), zinc acetate dehydrate (0.11 g), sodium selenite (0.086 g) and polyvinylpyrrolidone (0.4 g) were dissolved in a mixed solvent of EG and ED (24:1 volume ratio) under stirring for half an hour. Then the solution was transferred to a 50-mL Teflon-lined stainless steel autoclave and kept at 180 °C for 12 h. Thus, obtained precipitate was centrifuged and washed repeatedly with double-distilled water and ethanol. Finally, the synthesized RGO–ZnSe composites were dried in vacuum at 60 °C for 12 h. The controlled-ZnSe sample was also obtained following the identical experimental procedure in absence of GO.

2.3 Material Characterization

The crystal structure of the samples was characterized by an x-ray diffractometer (Rigaku Miniflex II) using Cu K_α radiation (λ = 1.54178 Å). Fourier transform infrared spectroscopy (FTIR) was recorded on spectrophotometer (Perkin Elmer Spectrum 100). The structural features and morphology were investigated by a scanning electron microscopy (SEM; Zeiss Merlin) and transmitting electron microscopy (TEM; JEOL-JEM 2100F), respectively. The photocatalytic activities of the as-synthesized ZnSe and RGO–ZnSe composite were evaluated from the decrement of the intensity of the absorption peak maxima the Rh B. The temperature was kept constant at 30 °C by circulating water surrounding the photoreactor. Twenty microliters of Rh B aqueous solution (concentration of 2 m mol L^{-1}) and 40 mL aqueous dispersion of RGO–ZnSe (concentration of 1.0 g L^{-1}) were taken in a photoreactor to evaluate the decomposition of the samples. The solution was magnetically stirred for 30 min under dark to get the adsorption–desorption equilibrium of Rh B. Then the solution was kept under simulated solar light illumination for 105 min. Three milliliters of the solution was withdrawn from the photoreactor in every 15-min intervals and followed by centrifugation to remove the catalyst. UV–Vis absorption spectra of the centrifuged solution were taken by a (Shimadzu UV-1700) UV–Vis spectrophotometer. The degradation of Rh B was studied by monitoring the decrease of major absorption peak of Rh B.

The degradation efficiency and the degradation rate constant were calculated as follows (Ref 12).

$$\text{Degradation efficiency } (\%) = \left(1 - \frac{C}{C_0}\right) \times 100\% \qquad \text{(Eq 1)}$$

where C_0 and C represent the concentration of Rh B at time 0 and t min, respectively.

The photodegradation rate constant was determined by the equation (Ref 12):

$$\ln\left(\frac{C_0}{C}\right) = kt \qquad \text{(Eq 2)}$$

where k (min^{-1}) is the degradation rate constant.

3. Results and Discussion

Figure 1(a) compares the diffraction patterns of graphite, GO, ZnSe, RGO and RGO–ZnSe composite. A sharp peak located at 2θ = 26.3° in the XRD pattern of graphite indicates the characteristic interlayer distance of 0.34 nm. After oxidation, graphitic peak completely disappears, while a broad peak centered at 2θ = 10.4° is appeared, confirms the formation of GO with d-spacing of 0.85 nm. The controlled-ZnSe and RGO–ZnSe composites reveal similar diffraction pattern with peaks corresponding to (111), (220) and (311) planes of cubic zinc blende [ZB] structured ZnSe [JCPDS card no. 37163] (Ref 4). In RGO–ZnSe composite, the peak of GO centered at 2θ = 10.4° disappears and the peak position of ZnSe remains unaltered which ruled out the possibility of formation of any other crystalline impurities in the composite.

The reduction in GO and formation of RGO–ZnSe composite was confirmed by FTIR spectroscopy. The FTIR transmission spectra of GO, ZnSe and RGO–ZnSe are displayed in Fig. 1(b). The absorption band located at 1618 cm^{-1} is assigned to skeletal vibrations of non-oxidized graphitic domains (C=C stretching), 1725 cm^{-1} is assigned to stretching vibration of –C=O, 1230 cm^{-1} is assigned to C–O, and 1047 cm^{-1} is assigned to C–O–C vibration observed in the FRIR transmission spectra of GO (Ref 13). The broad absorption band located at around 3400 cm^{-1} is assigned to the stretching vibration of O–H of absorbed H_2O molecules present in GO (Ref 13). The peaks of oxygen containing groups (–C=O, C–O and C–O–C) completely disappeared in the FTIR

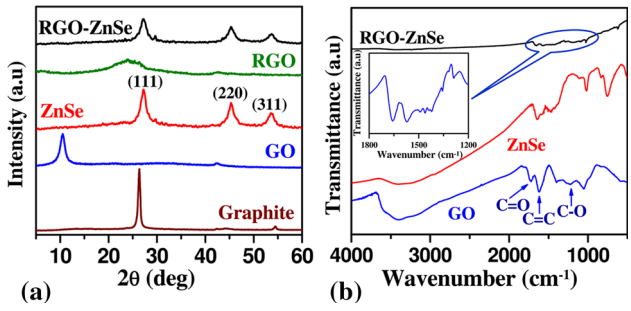

Fig. 1 (a) The XRD patterns of Graphite, GO, controlled-ZnSe, RGO and RGO–ZnSe composite. (b) FTIR spectra of GO, controlled-ZnSe and RGO–ZnSe composite. The magnified view of FTIR spectra of RGO–ZnSe composite is shown in the inset

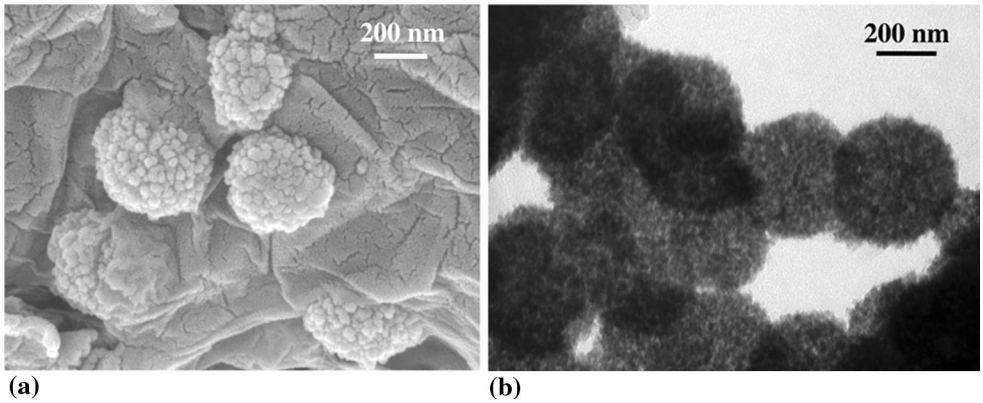

Fig. 2 (a) SEM and (b) TEM images of RGO–ZnSe composite

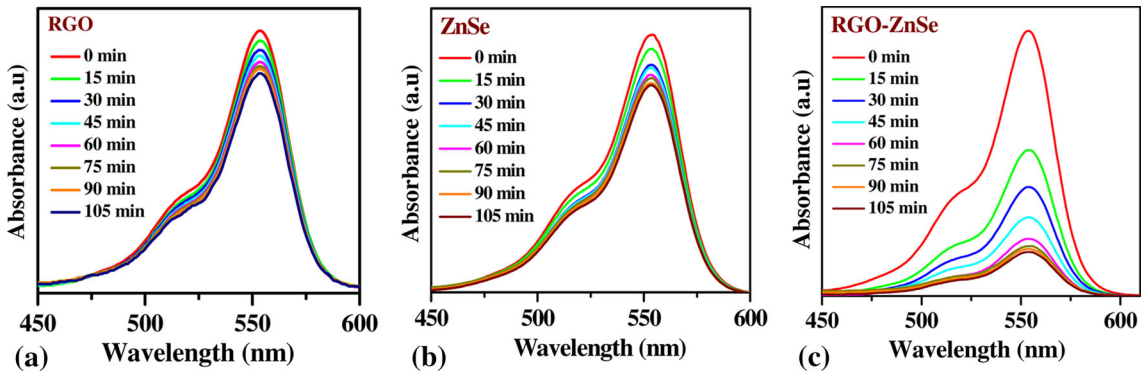

Fig. 3 UV–Vis absorption spectra of Rh B with (a) RGO, (b) controlled-ZnSe, (c) RGO–ZnSe composite for different time of simulated solar light illumination

spectra of RGO–ZnSe composite, indicating reduction in GO (Ref 13-15).

The morphological and microstructural details of RGO–ZnSe composite were examined by SEM and TEM imaging and are presented in Fig. 2(a) and (b), respectively. Well-distributed ZnSe microspheres consist with basic nanocrystals are clearly observed on the RGO sheets.

The photocatalytic activities of the RGO–ZnSe composite were evaluated by degradation of Rh B (as organic pollutant) under simulated solar light irradiation. Figure 3(a), (b) and (c) shows the UV–Vis absorbance spectra of aqueous solution of Rh B after photocatalytic degradation by RGO, controlled-ZnSe and RGO–ZnSe composite, respectively, within the time span from 0 to 105 min, with 15-min interval. It is observed that for both the cases the peak intensity of Rh B decreases with increasing time under the illumination of light, whereas it remains unaffected in darkness. After 105 min of illumination 83% of Rh B is degraded in presence of RGO–ZnSe composite, whereas only 16 and 18% of Rh B are degraded in presence of RGO and controlled-ZnSe, respectively, under identical experimental condition. The photodegradation efficiency of RGO, controlled-ZnSe and RGO–ZnSe composite with function of illumination time is compared in Fig. 4(a). The variation of $\ln(C/C_0)$ with illumination time (t) for RGO, controlled-ZnSe and RGO–ZnSe composite is shown in Fig. 4(b). A linear variation of $\ln(C/C_0)$ with illumination time is observed, which establishes the occurrence of pseudo-first-order photocatalytic degradation reaction (Ref 12-15). The degradation rate constant (k) of RGO–ZnSe photocatalyst is calculated as 0.025 min^{-1}, which is 12.5 times higher than RGO and controlled-ZnSe. The stability of the photodegradation efficiency of RGO–ZnSe composite has also been examined by studying its photodegradation efficiency over five cycles under identical experimental condition and is presented in Fig. 4(c). Our result depicts that the recycle use of the RGO–ZnSe composite does not considerably affect photocatalytic efficiency. We have also observed that phase and structure of RGO–ZnSe composite remain unaffected after photocatalytic cycles; establishing the stability of the catalyst for recycled use.

After illumination of light upon ZnSe, excitons are generated, which dissociates into free electrons and holes. Due to the favorable energy levels of conduction band of ZnSe and chemical potential of RGO, the photoinduced electron easily transfers to RGO sheets, leaving the hole at the valence band of ZnSe. These well-separated electrons and holes produce $OH^{\cdot}$ (hydroxyl radicals), the key factor for degrading Rh B and other organic dyes (Ref 12, 21-25). In RGO-based composite, RGO sheets act as solid state electron accepters, which enhance charge separation and subsequently increase the photocatalytic activities of the composite. The anticipated photocatalytic degradation mechanism of Rh B by RGO–ZnSe composite is presented in Fig. 4(d), and the mechanism for formation of $OH^{\cdot}$ is summarized below:

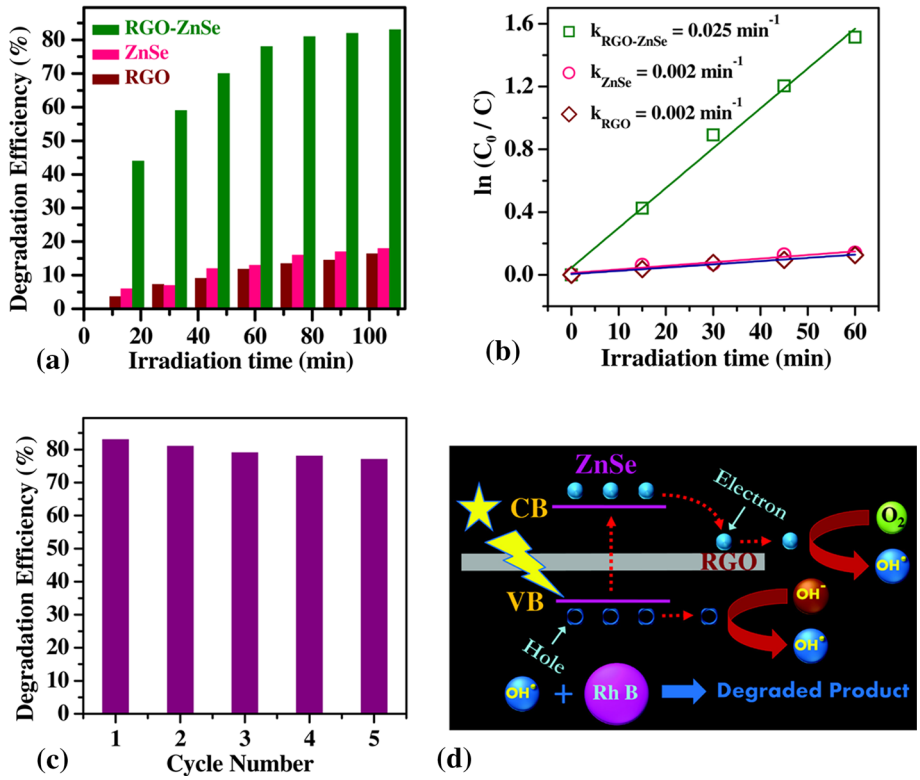

Fig. 4 (a) The comparison of the photodegradation efficiency and (b) plot of ln(C_0/C) as a function of time (t) under simulated solar light irradiation over RGO, controlled-ZnSe and RGO–ZnSe composite. (c) Photodegradation efficiency of RGO–ZnSe composite for different degradation cycle (d) schematic diagram of charge carrier transfer from ZnSe to RGO sheets and Rh B degradation mechanism under simulated solar light irradiation

$$\mathrm{ZnSe} + h\nu \rightarrow \mathrm{ZnSe}\,(e^- + h^+)$$
$$\mathrm{RGO} - \mathrm{ZnSe}\,(e^-) \rightarrow \mathrm{RGO}\,(e^-) + \mathrm{ZnSe}\,(h^+)$$
$$\mathrm{RGO}\,(e^-) + O_2 \rightarrow O_2^{-\cdot}$$
$$\mathrm{RGO}(e^-) + O_2^{-\cdot} + H^+ \rightarrow HO_2^-$$
$$HO_2^- + H^+ \rightarrow H_2O_2$$
$$H_2O_2 + e^- \rightarrow OH^{\cdot} + OH^-$$
$$\mathrm{ZnSe}\,(h^+) + H_2O \rightarrow OH^{\cdot} + H^+ + \mathrm{ZnSe}$$
$$OH^{\cdot} + \mathrm{Rh\,B} \rightarrow \mathrm{Degraded\ Product}.$$

4. Conclusions

In summary, we have successfully synthesized RGO–ZnSe composite by simple solvothermal process. The synthesized composite has been characterized structurally and morphologically by XRD, SEM and TEM image analysis. Well-distributed ZnSe microspheres consist with basic nanocrystals and are clearly observed on the RGO sheets. The reduction in GO is confirmed by FTIR spectroscopy study, where we have observed that all the oxygenated peaks disappears after the reduction in GO. Under identical experimental condition, the photodegradation efficiency and the photocatalytic rate constant have been increased by 4.6 and 12.5 times, respectively, in compared to controlled-ZnSe. In RGO-based composite system, RGO plays a crucial role to efficient charge separation, which enhanced the photocatalytic activity of the composite by hindering the electron–hole recombination inside ZnSe.

Acknowledgment

This work was supported by the Department of Science and Technology (DST), New Delhi, India, via Grant SR/FTP/PS-113/2010. We are also thankful to the University Grants Commission (UGC), and DST, New Delhi, India, for providing special assistance and infrastructural support to the Department of Physics and Technophysics, Vidyasagar University, via SAP and FIST program, respectively.

References

1. C. Chen, W. Ma, and J. Zhao, Semiconductor-Mediated Photodegradation of Pollutants Under Visible-Light Irradiation, *Chem. Soc. Rev.*, 2010, **39**, p 4206–4219
2. S.U.M. Khan, M. Al-Shahry, and W.B. Ingler, Efficient Photochemical Water Splitting by a Chemically Modified n-TiO_2, *Science*, 2002, **297**, p 2243–2245
3. L. Yang, J. Zhu, and D. Xiao, Microemulsion-Mediated Hydrothermal Synthesis of ZnSe and Fe-Doped ZnSe Quantum Dots with Different Luminescence Characteristics, *RSC Adv.*, 2012, **2**, p 8179–8188
4. S. Sarkar, S. Acharya, A. Chakraborty, and N. Pradhan, Zinc Blende 0D Quantum Dots to Wurtzite 1D Quantum Wires: The Oriented Attachment and Phase Change in ZnSe Nanostructures, *J. Phys. Chem. Lett.*, 2013, **4**, p 3292–3297
5. H. Kim, J. Kim, W. Kim, and W. Choi, Enhanced Photocatalytic and Photoelectrochemical Activity in the Ternary Hybrid of CdS/TiO_2/WO_3 through the Cascadal Electron Transfer, *J. Phys. Chem. C*, 2011, **115**, p 9797–9805
6. Y. Yin, Z. Jin, and F. Hou, Enhanced Solar Water-Splitting Efficiency using Core/Sheath Heterostructure CdS/TiO_2 Nanotube Arrays, *Nanotechnology*, 2007, **18**, p 495608

7. C.-H. Liu, Y.-C. Chang, T.B. Norris, and Z. Zhong, Graphene Photodetectors with Ultra-Broadband and High Responsivity at Room Temperature, *Nat. Nanotechnol.*, 2014, **9**, p 273–278
8. F. Bonaccorso, Z. Sun, T. Hasan, and A.C. Ferrari, Graphene Photonics and Optoelectronics, *Nat. Photon.*, 2010, **4**, p 611–622
9. S. Bae, H. Kim, Y. Lee, X. Xu, J.-S. Park, Y. Zheng, J. Balakrishnan, T. Lei, H.R. Kim, Y. Song, Y.-J. Kim, K.S. Kim, B. Ozyilmaz, J.-H. Ahn, B.H. Hong, and S. Iijima, Roll-to-roll Production of 30-Inch Graphene Films for Transparent Electrodes, *Nat. Nanotechnol.*, 2010, **5**, p 574–578
10. H. Feng, R. Cheng, X. Zhao, X. Duan, and J. Li, A Low-Temperature Method to Produce Highly Reduced Graphene Oxide, *Nat. Commun.*, 2013, **4**, p 1539
11. P.D. Tran, S.K. Batabyal, S.S. Pramana, J. Barber, L.H. Wong, and S.C.J. Loo, A Cuprous Oxide–Reduced Graphene Oxide (Cu_2O–rGO) Composite Photocatalyst for Hydrogen Generation: Employing rGO as an Electron Acceptor to Enhance the Photocatalytic Activity and Stability of Cu_2O, *Nanoscale*, 2012, **4**, p 3875–3878
12. S. Chakrabarty, K. Chakraborty, A. Laha, T. Pal, and S. Ghosh, Photocurrent Generation and Conductivity Relaxation in Reduced Graphene Oxide $Cd_{0.75}Zn_{0.25}S$ Nanocomposite and Its Photocatalytic Activity, *J. Phys. Chem. C*, 2014, **118**, p 28283–28290
13. K. Chakraborty, S. Chakrabarty, P. Das, S. Ghosh, and T. Pal, UV-Assisted Synthesis of Reduced Graphene Oxide Zinc Sulfide Composite with Enhanced Photocatalytic Activity, *Mater. Sci. Eng. B*, 2016, **204**, p 8–14
14. S. Ibrahim, S. Chakrabarty, S. Ghosh, and T. Pal, Reduced Graphene Oxide/Copper Phthalocyanine Composite and Its Optoelectrical Properties, *ChemistrySelect*, 2017, **2**, p 537–545
15. P. Das, K. Chakraborty, S. Chakrabarty, S. Ghosh, and T. Pal, Reduced Graphene Oxide–Zinc Sulfide Composite for Solar Light Responsive Photo Current Generation and Photocatalytic 4-Nitrophenol Reduction, *ChemistrySelect*, 2017, **2**, p 3297–3305
16. K. Chakraborty, S. Chakrabarty, T. Pal, and S. Ghosh, Synergistic Effect of Zinc Selenide—Reduced Graphene Oxide Towards Enhanced Solar-Light-Responsive Photo Current Generation and Photocatalytic 4-Nitrophenol Degradation, *N. J. Chem.*, 2017, **41**, p 4662–4671
17. B. Liu, L. Tian, and Y. Wang, One-Pot Solvothermal Synthesis of $ZnSe{\cdot}xN_2H_4$/GS and ZnSe/N-GS and Enhanced Visible-Light Photocatalysis, *ACS Appl. Mater. Interfaces*, 2013, **5**, p 8414–8422
18. P. Chen, T.Y. Xiao, H.H. Li, J.J. Yang, Z. Wang, H.B. Yao, and S.H. Yu, Nitrogen-Doped Graphene/ZnSe Nanocomposites: Hydrothermal Synthesis and Their Enhanced Electrochemical and Photocatalytic Activities, *ACS Nano*, 2012, **6**, p 712–719
19. S.H. Hsieh, W.J. Chen, and T.H. Yeh, Degradation of Methylene Blue using ZnSe-Graphene Nanocomposites Under Visible-Light Irradiation, *Ceram. Int.*, 2015, **41**, p 13759–13766
20. W.S. Hummers and R.E. Offeman, Preparation of Graphitic Oxide, *J. Am. Chem. Soc.*, 1958, **80**, p 1339
21. W. Liu, M. Wang, C. Xu, S. Chen, and X. Fu, Ag_3PO_4/ZnO: An Efficient Visible-Light-Sensitized Composite with Its Application in Photocatalytic Degradation of Rhodamine B, *Mater. Res. Bull.*, 2013, **48**, p 106–113
22. Q.I. Rahman, M. Ahmad, S.K. Misra, and M. Lohani, Effective Photocatalytic Degradation of Rhodamine B Dye by ZnO Nanoparticles, *Mater. Lett.*, 2013, **91**, p 170–174
23. N. Zhang, M.-Q. Yang, S. Liu, Y. Sun, and Y.-J. Xu, Waltzing with the Versatile Platform of Graphene to Synthesize Composite Photocatalysts, *Chem. Rev.*, 2015, **115**, p 10307–10377
24. M.-Q. Yang, N. Zhang, M. Pagliaro, and Y.-J. Xu, Artificial Photosynthesis over Graphene–Semiconductor Composites. Are We Getting Better?, *Chem. Soc. Rev.*, 2014, **43**, p 8240–8254
25. U.G. Akpan and B.H. Hameed, Parameters Affecting the Photocatalytic Degradation of Dyes Using Tio_2-Based Photocatalysts: A Review, *J. Hazard. Mater.*, 2009, **170**, p 520–529